

Critical magnetic fluctuations induced superconductivity and residual density of states in $CeRhIn_5$ superconductor

Yunkyu Bang^{1,2,3}, I. Martin² and A.V. Balatsky²

¹ Department of Physics, Chonnam National University, Kwangju 500-757, Korea

² Theoretical Division Los Alamos National Laboratory, Los Alamos, New Mexico 87545

³ Center for Strongly Correlated Materials Research, Seoul National University, Seoul 151-742, Korea
(February 1, 2008)

We propose the multiband extension of the spin-fermion model to address the superconducting d-wave pairing due to magnetic interaction near critical point. We solve the unrestricted gap equation with a general d-wave symmetry gap and find that divergent magnetic correlation length ξ leads to the very unharmonic shape of the gap function with shallow gap regions near nodes. These regions are extremely sensitive to disorder. Small impurity concentration induces substantial residual density of states. We argue that we can understand the large $N_{res}(0) = \lim_{T \rightarrow 0} C_p(T)/T$ value and its pressure dependence of the recently discovered $CeRhIn_5$ superconductor under pressure within this approach.

PACS numbers: 74.20, 74.20-z, 74.50

Recent discovery of superconductivity in $CeMIn_5$ ($M = Co, Rh, Ir$)^{1,2} has spurred renewed interest of heavy fermion systems and about the nature of its superconductivity. The rich phase diagram of these compounds and the tunability by pressure and chemical substitution of the transition metal elements³ provide valuable information about the competition/interplay between the magnetism and superconductivity and perhaps a possible quantum criticality as a unifying origin of the phase diagram of these compounds⁴. While the complete understanding of the phase diagram and the underlying mechanism for the magnetism and the superconductivity is still lacking, there are many details of thermodynamic and transport properties of each phase in these materials which need to be understood: large remnant $N_{res}(0) = \lim_{T \rightarrow 0} C_p(T)/T$ values both in magnetic and in superconducting phases⁵, the weak first order transition to superconductivity in $CeRhIn_5$ ⁵, a unidentified new phase inside the mixed state⁶, a strong deviation of $\Delta C(T_c)/C(T_c)$ from BCS value and its pressure dependence^{5,7} etc.

Motivated by $CeRhIn_5$ experiment⁵, in this paper we examined possible conditions for a d-wave superconductors (1) to create a substantial density of states (DOS) in superconducting phase with a small impurity concentration, and (2) to have a large variation of it as a function of pressure while keeping the constant T_c ⁵.

The $N_{res}(0)$ value at 16.5 kbar seen experimentally is almost half of the normal state $N(0)$ ⁵. From the previous studies⁸, it is required to have a large amount of impurities in order to create large $N_{res}(0)$ by magnetic/nonmagnetic isotropic impurity in the superconducting state with lines of nodes⁹ (the normal state scattering rate Γ should be about $\Gamma/\Delta_0 \geq 0.5$ with Born scatterer and $\Gamma/\Delta_0 \geq 0.1$ with a unitary scatterer¹⁰). Even more intriguing is the pressure dependence of $N_{res}(0)$; it varies from almost the half of the normal state $N(0)$ at 16.5 kbar to almost zero value at 21 kbar in one sample.

Assuming a simple form of d-wave paring $\Delta_0(\cos(k_x) - \cos(k_y))$, such a large variation of $N_{res}(0)$ in the same sample requires extremely sharp increase of Δ_0 with increasing pressure. This would be difficult to reconcile with almost constant T_c values between 16 \sim 21 kbar⁵.

To address these questions we need a microscopic model for the superconducting state in $CeMIn_5$ materials. From the phase diagram of these materials¹⁻⁵ and from the thermal conductivity measurement indicating the unconventional pairing with lines of nodes⁹, we argue that it is highly plausible that *the superconductivity is mediated by the magnetic fluctuations*^{4,11}. We propose a multiband generalization of the spin-fermion model¹² where localized Ce spins \vec{S} are interacting with the conduction electrons (predominantly d band of In) via the Kondo exchange coupling J . In mixed momentum and real space representation the Hamiltonian is written as

$$H = \sum_{\mathbf{k}, \alpha} c_{\alpha}^{\dagger}(\mathbf{k}) \varepsilon(\mathbf{k}) c_{\alpha}(\mathbf{k}) + \sum_{\mathbf{r}, \alpha, \beta} J \vec{S}(\mathbf{r}) \cdot c_{\alpha}^{\dagger}(\mathbf{r}) \vec{\sigma}_{\alpha \beta} c_{\beta}(\mathbf{r}) + H_S \quad (1)$$

where the first term is a kinetic energy and the second describes the Kondo exchange between Ce spins and conduction electron spin density. The last term represents an effective low energy Hamiltonian for the localized spins. The dynamics of the localized spins without long range AFM order coupled with conduction electrons is well captured by the spin correlation function¹³⁻¹⁵, $\chi(\mathbf{q}, \omega) = \delta_{ij} \langle S^i(\mathbf{q}, \omega) S^j(\mathbf{q}, -\omega) \rangle = \frac{V_0}{i\omega/\omega_0 + \xi^{-2}(\mathbf{q} - \mathbf{Q})^2 + 1}$, where ω_0 is a spin relaxation energy scale, \mathbf{Q} is the 2-dimensional antiferromagnetic vector, and ξ is the magnetic correlation length. The physics of this model for a one band case has been investigated for a long time^{14,15}. It is important to mention that the spin-fermion model of our multiband case is different in the following aspects: (1) the effective spin-fermion coupling should be much

weaker¹² than that of the one band model. One important consequence of it is that the relaxational energy scale ω_0 is much larger than that of the one band case ω_{sf} ^{13,15}; (2) more importantly, while the $\xi \gg a$ limit can not be reached in the self-consistent one band model without deforming the FS topology of the conduction band¹⁶, in the two band model in conjunction with the weak coupling above mentioned, the $\xi \gg a$ limit doesn't necessarily modify the conduction band Fermi surface¹²; (3) below T_c , however, the spin fluctuation damping ω_0 is suppressed for $\omega < 2\Delta_{sc}$, thus modifying the spin fluctuations spectrum. This effect should be dealt with in the fully self-consistent Eliashberg equation. In our weak coupling BCS approximation, this effect is ignored and justified by the fact $\Delta_{sc} < \omega_0$ *a posteriori*.

The phase diagram for this material⁵ suggests that ξ becomes gradually shorter away from the phase boundary ($P_c \sim 15\text{kbar}$) toward the higher pressure. Then the basic feature of the magnetic fluctuations mediated potential is that near critical point with divergent ξ $V(\mathbf{q}) \equiv \chi(\mathbf{q}, \omega = 0)$ is sharply peaked around the antiferromagnetic wave vector $\vec{\mathbf{q}} \sim \vec{\mathbf{Q}}$ without much tail at other \vec{q} values. With this potential the d-wave gap becomes mostly confined near the antinodal points and the gap in the nodal regions becomes shallow¹⁷. Upon decreasing the correlation length ξ , the potential has a longer tail extending outside the $\vec{\mathbf{Q}}$ vector. As a result the gap function approaches a simple harmonic function $\sim (\cos(k_x) - \cos(k_y))$ with a constant slope of the gap over most of the Fermi surface (FS). In this paper we show that the OP slope of the nodal region is very sensitive to the shape of the pairing potential (see Fig.1(a)-(b)) and the shallow gap near nodal points leads to the enhanced sensitivity to disorder so that only small amount of impurities is required to produce substantial residual DOS $N_{res}(0)$. To capture this detailed shape of the d-wave OP, we solved the unrestricted gap equation with only keeping the general d-wave symmetry. Then we study the impurity effects using T-matrix approximation to calculate the impurity-induced DOS $N_{res}(\omega)$ in the superconducting state.

Formalism. For $CeRhIn_5$ we assume $\Delta_0 < \omega_0$. This allows us to use a weak coupling BCS gap equation of the spin-fermion model for the d-wave pairing¹⁴. For simplicity, we assume a circular FS in two dimensions and integrate out the perpendicular component of momentum up to the BCS cut-off energy ω_D , which is naturally provided by ω_0 in our model. The effect of the impurity scattering is included within T-matrix approxiamtion⁸. For particle-hole symmetric case $T_3 = 0$, and for d-wave OP with isotropic scattering $T_1 = 0$ (also without loss of generality we can choose $T_2 = 0$ by U(1) symmetry). Then we need to calculate only $T_0(\omega)$. Self energy is given $\Sigma_0 = \Gamma T_0$, where $\Gamma = n_i/\pi N_0$, N_0 the normal DOS at the Fermi energy, n_i the impurity concentration. Scattering strength parameter c is related with the s-wave phase shift δ as $c = \tan^{-1}(\delta)$. Now $T_0(\omega_n) = \frac{g_0(\omega_n)}{[c^2 - g_0^2(\omega_n)]}$, where

$g_0(\omega_n) = \frac{1}{\pi N_0} \sum_k \frac{i\omega_n}{\tilde{\omega}_n^2 + \epsilon_k^2 + \Delta(k)}$, $\tilde{\omega}_n = \omega_n + \Sigma_0$. With this T_0 the following gap equation is solved self-consistently.

$$\Delta(\phi) = -N_0 \int \frac{d\phi'}{2\pi} V(\phi - \phi') \cdot F(\phi') \cdot T \sum_{\omega_n} \int_{-\omega_D}^{\omega_D} d\epsilon \frac{\Delta(\phi')}{\tilde{\omega}_n^2 + \epsilon^2 + \Delta(k)}. \quad (2)$$

Unlike the previous calculations of d-wave pairing, we assume no particular functional form for $\Delta(\phi)$ except imposing D_2 symmetry; namely $\Delta(n\pi/4) = 0$ ($n = 1, 3, 5, 7$), $\Delta(\phi) = \Delta(\phi \pm \pi)$, and $\Delta(\phi) = -\Delta(\phi \pm \pi/2)$. Therefore the gap equation can produce the most general d-wave symmetry gap solution for a given pairing potential. The pairing potential is proportional to the static limit of $\chi(\mathbf{q}, \omega = 0) \sim \frac{1}{(q - Q)^2 + \xi^{-2}}$, which is parameterized as follows.

$$V(\delta\phi) = V_d(b) \frac{b^2}{(\delta\phi \pm \pi/2)^2 + b^2}. \quad (3)$$

where the Lorenzian part is normalized and $V_d(b)$ determines the total coupling strength. Apparently the parameter b is proportional to ξ^{-1} , normalized in the circular Fermi surface ($\xi \sim a\pi/b$; a is the lattice parameter). Both ξ and $V_d(b)$ are functions of pressure. We numerically determine $V_d(b)$ to make T_c constant in accord with $CeRhIn_5$ experiment⁵. Finally, we introduce the FS weighting function $F(\phi) = \cos^\beta(2\phi)$ to correct the artifact of the circular FS and to mimic the important aspect of real FS topology¹⁸.

Results. In all calculations we use $\omega_D = 1$, which also serves the unit energy. In Fig.1(a) we show the normalized pairing potentials $V(\phi)/V_d(b)$ as a function of b for illustration. In Fig.1(b) the solutions of $\Delta(\phi)$ for the Born limit scatterer ($c = 1, \Gamma = 0.05$) are shown for the potentials shown in Fig.1(a).

The self-consistently determined $T_0(\omega_n)$ is analytically continued to real frequency using Pade approximant¹⁹ to calculate the self-energy ($\Sigma_0(\omega + i\eta)$). Then $N(0) = \frac{1}{\pi} \sum_k \text{Im}G_0(\omega, k)$ is calculated. In Fig.2.a-b we plot $\text{Im}\Sigma_0(\omega)$ for both Born and unitary limits for potentials with different $b \sim \xi^{-1}$ shown in Fig.1. There is no resonance at Fermi level for Born limit scatterer as known, but the scattering rate $\gamma = \text{Im}\Sigma_0(\omega = 0)$ increases as the gap of nodal region becomes flatter, and for all cases for $|\omega| > \Delta_0$ it approaches the normal scattering rate $\Gamma_N = \Gamma/(c^2 + 1) = 0.025$. As a result the residual DOS $N_{res}(\omega = 0)$ (see the Fig.3.a) sharply increases with flatter gap region. On the other hand, for the case of unitary scatterer (Fig.2.b) there is a resonance at the Fermi level for all cases, but the strength of this scattering rate γ has opposite trend in contrast to the Born limit; the flatter the gap is, the smaller γ is. This is because the self-consistent equations are different for each case: $\gamma = \Gamma n_0/c^2$ for Born limit and $\gamma = \Gamma/n_0$ for unitary limit ($n_0 = \langle \frac{\gamma}{\sqrt{\gamma^2 + \Delta(\phi)}} \rangle$). Also for $|\omega| > \Delta_0$ it

approaches the normal scattering rate $\Gamma_N = \Gamma = 0.005$. Nevertheless for both cases even small value of γ is sufficient to create the substantial $N_{res}(0)$ at Fermi level when the gap is shallow near nodes. This is seen in Fig.3.a-b which plots the normalized DOS, $N(\omega)/N_0$, for both Born and the unitary limits. The clearly seen trend is that the longer magnetic correlation ξ produces a more residual DOS, $N(\omega)/N_0$ for a same amount of impurities.

Fig.4(a) summarizes this trend, shows plots of $N(\omega = 0)/N_0$ as a function of b ($\sim P$) for both impurity cases. The result shows that the Born limit scatterer has a stronger dependence on pressure compared to the unitary scatterer. This is because of the opposite trend of γ in unitary scatterer due to the resonant pole. In comparison to the experimental data of $N_{res}(0)$ ⁵(shown in Fig.4(b)), the Born scatterer fits the data better.

In Fig.5 we show T_c suppression as a function of impurity scattering parameter Γ for both Born ($c = 1$) and unitary ($c = 0$) limits for the representative potentials ($b = 0.1$). The impurity scattering parameters used in our calculations gives $(T_c(\Gamma) - T_{c0})/T_{c0}$ suppression of at most a few % from Fig.5.(unitary limit 0.8%, Born limit 4%). In passing we note Γ_{crit}/Δ_0 is about 50% larger than the simple $\cos(2\phi)$ type d-wave result⁸ both for Born and the unitary cases. This means that the unrestricted gap equation can find a more optimized gap solution up to higher temperature compared to the fixed form of $\Delta_0 \cos(2\phi)$ solution.

In summary, in this paper, we propose a multiband spin-fermion model as a description of the pairing in $CeMIn_5$ materials. Motivated by the phase diagram of these materials, we assume that the magnetic correlation length ξ decreases with pressure and the functional shape of the magnetic fluctuations mediated pairing potential is changing. Using this potential we show that the slope of the gap near nodes can be sharply changed. This strong change of the slope can explain the pressure dependence of $N_{res}(0)/N_0$ as well as the large value of it in $CeRhIn_5$ superconductor⁵ close to the quantum critical limit of $\xi \rightarrow \infty$ with a small amount of impurity.

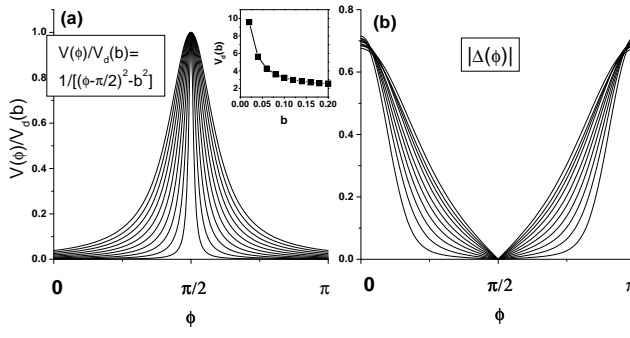


FIG. 1. (a) The normalized pairing potential $V(\phi)/V_d(b)$ as a function of the exchange momentum ϕ , for different values of b ($\sim \xi^{-1}$). In increasing order of potential width, $b=0.02, 0.04, \dots, 0.2$. $\phi = \pi/2$ is the AFM peak momentum \vec{Q} . Inset is the $V_d(b)$ which is numerically determined to make T_c constant. The trend is that the potential height is decreasing as ξ becomes shorter (or the pressure increases) and the width is increasing. (b) The OP solutions $\Delta(\phi)$ for pairing potentials shown in (a) with impurities (Born limit $c = 1$ and $\Gamma = 0.05$) for all cases. In decreasing order of potential width, $\Delta(\phi)$ becomes flatter near node. This trend of the flatter gap near node approaching the magnetic phase (the longer ξ) is also observed in the high T_c superconductors²⁰.

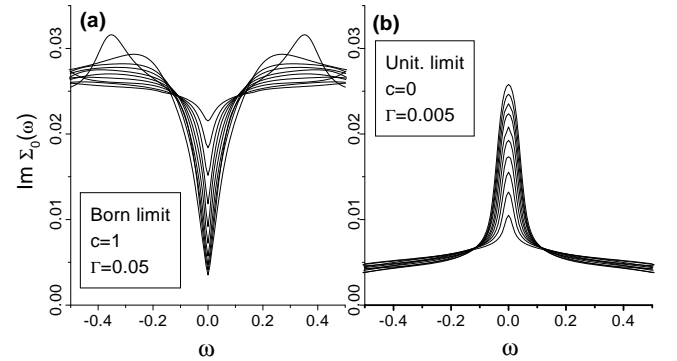


FIG. 2. (a) The imaginary part of self-energy $Im\Sigma_0(\omega)$ for different pairing potentials shown in Fig.1. with Born limit scatterer ($c = 1$ and $\Gamma = 0.05$). With increasing potential width, $\gamma = Im\Sigma_0(\omega = 0)$ decreases.; (b) the same as (a) with the unitary scatterer ($c = 0$ and $\Gamma = 0.005$). With increasing potential width, γ increases.

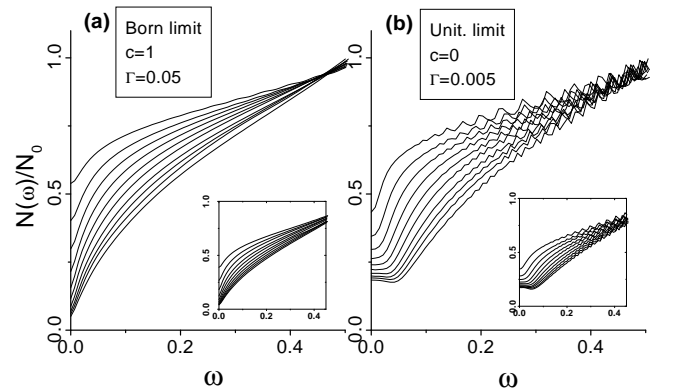


FIG. 3. (a) The normalized DOS $N(\omega)/N_0$ for different pairing potentials as shown in Fig.1. with Born limit scatterer ($c = 1$ and $\Gamma = 0.05$). With increased potential width $N(\omega)/N_0$ decreases. Inset: with $\beta = 4$ and $\Gamma = 0.06$. (b) the same as (a) with the unitary scatterer ($c = 0$ and $\Gamma = 0.005$). With increased potential width $N(\omega)/N_0$ decreases. Inset: with $\beta = 4$ and $\Gamma = 0.006$.

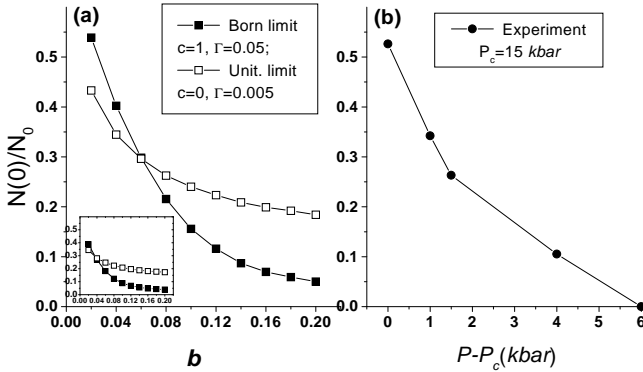


FIG. 4. (a) The normalized DOS $N(\omega = 0)/N_0$ as a function of b ($\sim \xi^{-1} \sim P - P_c$) for Born limit scatterer ($c = 1$, $\Gamma = 0.05$, solid square) and for the unitary scatterer ($c = 0$, $\Gamma = 0.005$, open square). Inset is with $\beta = 4$ ($c = 1$, $\Gamma = 0.06$, solid square; $c = 0$, $\Gamma = 0.006$, open square); (b) Experimental data from Ref[5].

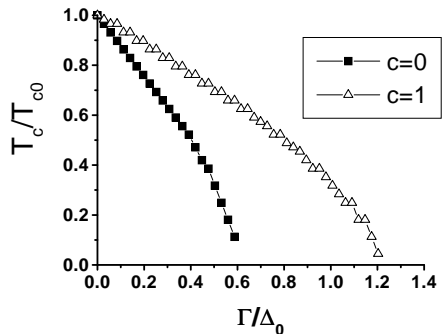


FIG. 5. T_c/T_{c0} as a function of Γ/Δ_0 both for the Born ($c = 1$) and unitary limit ($c = 0$) with a typical paring potential ($b = 0.1$).

We are grateful to R. Movshovich, J. Thompson, J. Sarrao, Ar. Abanov for useful discussions. This work was supported by US DoE. Y.B. was partially supported by the Korean Science and Engineering Foundation (KOSEF) through the Center for Strongly Corre-

lated Materials Research (CSCMR) (2001) and through the Grant No. 1999-2-114-005-5.

- ¹ H. Hegger et al., Phys. Rev. Lett. **84**, 4986 (2000).
- ² C. Petrovic et al., Europhys. Lett. **53**, 354 (2001); C. Petrovic et al., J. Phys. Condens. Matter **13**, L337 (2001).
- ³ P.G. Pagliuso et al., cond-mat/0107266.
- ⁴ N.D. Mathur et al., Nature **394** 39 (1998); S.S. Saxena et al., *ibid* **406** 587 (2000).
- ⁵ R. A. Fisher et al., cond-mat/0109221.
- ⁶ T. P. Murphy et al., cond-mat/0104179.
- ⁷ E. Lengyel et al., unpublished.
- ⁸ P. J. Hirschfeld and N. Goldenfeld, Phys. Rev. B **48**, 4219 (1993); R. Fehrenbacher and M. Norman, Phys. Rev. B **50**, 3495 (1994).
- ⁹ R. Movshovich et al., Phys. Rev. Lett. **86**, 5152 (2001).
- ¹⁰ If the data in Ref[5] were for a particular sample which happens to contain a large amount of impurities, any cleaner sample should easily have twice as large T_c . On the other hand the sample-to-sample variation of T_c of $CeRhIn_5$ is almost zero, so it means that the $T_c = 2.3K$ sample is a really intrinsic one.
- ¹¹ The specific heat data⁵ suggests that the transition from the AFM to SC is weakly first order, we think that this weak first order transition doesn't change the nature of the AFM fluctuations drastically in the SC phase.
- ¹² Clear experimental evidence for the necessity of the two band model is that the resistivity of $CeRhIn_5$ continues to be metallic and even decreased below T_N in the magnetic phase ($p < p_c$)¹. It implies that the long range magnetic order of Ce spins doesn't induce the concomitant SDW gap in the conduction band.
- ¹³ A.J. Millis, H. Monien, and D. Pines, Phys. Rev. B **42**, 167 (1990).
- ¹⁴ P. Monthoux, A. V. Balatsky, and D. Pines, Phys. Rev. Lett. **67**, 3448 (1991); Phys. Rev. B **46**, 14803 (1992); K. Miyake, S. Schmitt-Rink, and C. M. Varma, Phys. Rev. B **34**, 6554 (1986).
- ¹⁵ A. V. Chubukov, and D. Morr, Phys. Rep., **228**, 355 (1997) and references therein.
- ¹⁶ Jorg Schmalian, D. Pines, and B. Stojkovic, cond-mat/9804129.
- ¹⁷ Ar. Abanov, A. V. Chubukov, and A. M. Finkel'stein, Europhys. Lett. **54**, 488 (2001).
- ¹⁸ Because of the circular FS, the pairing potential $V(\phi - \phi')$ itself is invariant with the simultaneous shift of ϕ and ϕ' , and cannot distinguish the hot spots (parts of FS connected by the antiferromagnetic wave vector $\pm \vec{Q}$) and cold spots on the FS. Therefore it is essential to introduce the FS weight function to avoid the artifact of the circular FS. In this paper we use $F(\phi) = \cos^\beta(2\phi)$ with $\beta = 8$, but the results with $\beta = 4$ are not much different although it apparently produces less flat OP near nodes.
- ¹⁹ H.J. Vidberg and J.W. Serene, J. of Low Temp. Phys. **29**, 179 (1977).

²⁰ Z.-X. Shen (private communication)